Int. J. Electrochem. Sci., 15 **(2020)** 4840 – 4852, doi: 10.20964/2020.06.57

International Journal of
ELECTROCHEMICAL
SCIENCE
www.electrochemsci.org

Short Communication

Effects of Surface Characteristics of AISI 304 Stainless Steel by Wet Shot Peening and its Wear and Corrosion Behavior

Xinlong Wei[1], Dejia Zhu[1], Wuyan Zhu[1], Duoli Wu[1], Juan Li[2], Chao Zhang[1,]*

[1] School of Mechanical Engineering, Yangzhou University, Yangzhou 225127, China
[2] School of Mechanical and Electrical Engineering, Nanjing Forestry University, Nanjing 210037, China
[*]E-mail: zhangc@yzu.edu.cn

Received: 3 February 2020 / *Accepted:* 30 March 2020 / *Published:* 10 May 2020

In this paper, wet shot peening (WSP) is applied to investigate the influence on wear and corrosion behavior of AISI 304 stainless steel using dry reciprocating sliding wear tests and electrochemical impedance spectroscopy (EIS) experiments. Surface modifications including microstructure, surface roughness, microhardness and phase transformation are characterized. Results show that wet shot peening produces grain refinement because of intersection of deformation twins at different directions, increases surface roughness and generates martensite phase. Microhardness at the top surface can be enhanced significantly due to the strain hardening produced by WSP. Results of dry sliding wear tests reveal a remarkable improvement in wear resistance by WSP. The wear mechanism is a mixture of abrasive and adhesive wear for both as-received and wet shot peened AISI 304 stainless steel. Results of EIS experiments show that the charge transfer resistance of relative higher peening coverage WSP treated sample is higher than those of lower peening coverage WSP treated and as-received samples in the acid chloride solution at room temperature. The improved corrosion resistance for higher peening coverage WSP can be achieved by the positive combined action of grain refinement, surface roughness and deformation induced martensite.

Keywords: Wet shot peening, Corrosion resistance, Wear resistance, Electrochemical impedance spectroscopy, Microstructure, Deformation induced martensite

1. INTRODUCTION

Austenitic stainless steel is a kind of highly significant structural materials for their excellent mechanical properties and broad industrial application. Despite the inherent high corrosion resistance, this category of steel does not show a suitable resistance to local corrosion and wear [1-8]. Thus, there are demands to improve corrosion resistance and wear behavior of austenitic stainless steel in specific applications by surface modification technologies.

Researchers have developed many mechanical surface treatment techniques, such as laser shock processing [9-11], ultrasonic impact treatment [12], shot peening treatment [13-14]. Shot peening can be applied to increase wear behavior because of the improved surface hardness and mitigation of cracks initiation and propagation within the enhancement region [15-16]. Ganesh et al. [15] investigated the wear behavior of titanium alloys after shot peening. Results showed that shot peening enhanced wear resistance of titanium alloys by improving the surface hardness. Mitrovic et al. [16] reported that shot peening decreased the friction coefficient and wear rate in both dry and lubricated sliding conditions. However, there are contrasting studies in order to investigate whether shot peening actually increases the wear resistance of materials [17-18]. Zammit et al. [18] founded that the results of the wear factors and friction coefficients showed that shot peening did not improve the wear resistance.

Shot peening is a highly effective and common mechanical surface enhancement treatment to improve corrosion resistance of metallic workpieces by introducing severe plastic deformation into the near surface area. The three main characteristics of shot peened surface are limited roughening, refined microstructure and compressive residual stresses. Wang et al. [19] reported that surface nanocrystallization induced by shot peening could markedly enhance the corrosion resistance of 1Cr18Ni9Ti stainless steel in the chlorine-ion-contained solution. Chen et al. [20] investigated the effects of shot peening treatment on microstructure and corrosion behavior of 316LN stainless steel. Results showed that the microstructure with nanocrystallines and a high density of twins induced by shot peening could improve the uniformity and compactness of the passive film and produce a better corrosion resistance. Kovaci et al. [21] revealed that the corrosion resistance of the material increased with the increasing shot peening intensity because of grain refinement and formation of sub-grains. Nevertheless, the lack of knowledge on corrosion behavior after shot peening still exists. Reports on corrosion behavior modified by shot peening are inconsistent without showing an explicit trend [22-25]. Lee et al. [24] found that the shot peened specimen showed the lower corrosion resistance than the as-received specimen due to surface roughness and deformation induced martensite produced by shot peening. Zupanc and Grum [25] observed higher corrosion current density on the shot peened specimens by a factor of 2.5 compared to the as-machined specimens.

In this paper, wet shot peening is carried out to study the effects on corrosion and wear behavior of 304 stainless steel. Surface modifications, such as microstructure, surface roughness, microhardness and phase transformation are characterized. The effects of WSP on the tribological characteristics of stainless steel are examined by experiments in dry sliding condition. Furthermore, electrochemical impedance spectroscopy (EIS) is applied to investigate the influences of WSP on corrosion behavior of AISI 304 stainless steel in acidic chloride ion aqueous solution.

2. EXPERIMENTAL PROCEDURES

2.1 Specimens preparation

Samples were made from 3 mm thickness AISI 304 stainless steel plate. Table 1 showed the

chemical composition of materials. Before WSP, all the samples were polished with silicon carbide papers to 1000 grit, and subsequently cleaned in deionized water and ethanol.

Table 1. Chemical composition of AISI 304 stainless steel

Element	C	Si	Mn	S	P	Cr	Ni	N	Fe
Content (wt.%)	0.041	0.55	1.08	0.005	0.022	18.21	8.09	0.04	Balance

A mixture of 0.2 mm diameter ceramic balls and 10 wt.% water was used in wet shot peening experiments. The wet ceramic balls were propelled and accelerated into the blasting nozzle directed at the specimen by high pressure air. The 0.5 MPa peening pressure was set by controlling air compressor pressure. In addition, the distance between nozzle and the specimen was 100 mm and the incident angle was 90°. The coverage is defined as a percentage relating to the surface coverage of the sample, i.e. 100% coverage equates to one complete surface coverage of shot peening indents. Three coverages of 100%, 200% and 500% were used. At the end of WSP treatment, small square specimens with dimensions of 10 × 10 × 3 mm were obtained from the treated plate by means of electrical spark wire cutting, followed by cleaned in ethanol. Then, wear and corrosion test specimens were inserted in epoxy resin exposed with 1 cm^2 area.

2.2 Characterization

The cross-sectional microstructure near the top surface was observed by the field emission scanning electron microscope (SEM). The samples were sectioned near the affected area by WSP and carefully polished until none of scratches could be found on the surface. Then samples were etched using 10% oxalic acid aqueous solution for duration of 80 s at 3 V voltage.

Surface roughness before and after wet shot peening was carried out by using a surface profiler equipment. Arithmetic average roughness R_a value was obtained.

The XRD qualitative analysis of phase transformation caused by wet shot peening was carried out using Cu-Kα radiation on a X-ray diffraction equipment. The equipment was performed in condition of 40 kV and 40 mA. The 2θ range of 40-100° with a step by step scanning length of 0.02° was set to obtain the X-ray diffraction data. Using the 111, 200 reflections for austenite phase and the 110, 200 reflections for martensite phase, the volume fraction V_α of α-martensite phase at the top surface is estimated by Eq.1 in the following [26-27]:

$$V_\alpha = \frac{\frac{1}{n}\sum_{j=1}^{n}\frac{I_\alpha{}^j}{R_\alpha{}^j}}{\frac{1}{n}\sum_{j=1}^{n}\frac{I_\gamma{}^j}{R_\gamma{}^j}+\frac{1}{n}\sum_{j=1}^{n}\frac{I_\alpha{}^j}{R_\alpha{}^j}} \quad (1)$$

where n is the number of the phase peaks used in calculation, I is the integrated intensity of the reflecting plane and R is the material scattering factor.

Microhardness near the wet shot peened surface at the depth direction was measured on HV-

1000 Vickers hardness tester. The experiments were carried out 3 times in the same test location with 100 g load for 15 s duration.

2.3 Wear test procedure

Dry reciprocating sliding wear tests were conducted on steel samples using a Bruker UMT-2 tribometer with a ball-on-flat configuration with the normal loads of 5 N and 20 N. The reciprocating frequency, test duration and the sliding length were 4 Hz, 1 h and 5 mm, respectively. Si_3N_4 balls with a diameter of 4 mm were used as counterfaces in order to evaluate the wear behavior of samples with and without WSP, which were performed at room temperature with a 45%-55% relative humidity. Quantitative analysis of wear volume was carried out by measuring the cross sectional area in the wear tracks and converting this area into the wear volume. In order to minimize the data scattering, each test was conducted three times. The wear rate is obtained by Eq.2 as follows:

$$W_s = \frac{\Delta V}{F \cdot L} \tag{2}$$

Where ΔV is the wear volume, F is the applied normal force and L is the total sliding distance.

2.4 Electrochemical impedance spectroscopy (EIS) behavior

Electrochemical impedance spectroscopy (EIS) experiments were conducted by Gamry Interface1010E, in which the three-electrode configuration that a saturated calomel electrode (SCE) was used as the reference electrode and a platinum foil was used as the counter electrode was equipped with. Tests were conducted in the frequency range from 100 kHz to 0.05 Hz, in which the 10 mV AC amplitude was superimposed versus the obtained open circuit potential. The environment was 3.5% NaCl + 0.2 mol/L HCl solution at room temperature.

3. RESULTS AND DISCUSSION

3.1 Microstructure characteristics

Surface microstructure characteristics of grains for specimens before and after WSP are shown in Figure 1. Single γ-austenite microstructure is visible in the as-received specimen. At the top surface of wet shot peened specimens, deformation twins caused by severe plastic deformation are clearly observed. Similar deformation microstructure characteristics are observed by Jayalakshmi et al. [28]. The number of deformation twins directions increases with the increase of peening coverage. In Figure 1b, the intersection of deformation twins at three directions is shown in area C and occurs in depth of about 15 μm depth from the top surface in the wet shot peened area, which splits the original coarse austenitic grains into plenty of submicron triangular blocks. As the depth increases, the number of deformation twins direction reduces. In other words, both deformation twins at two directions shown in area B and a single direction shown in area A occur, splitting the original coarse austenitic grains

into submicron rhombic blocks and parallel small platelets, respectively. The increase of peening coverage of WSP improves surface cumulative plastic strain, after 500% coverage wet shot peening treatment, the area of deformation twins intersection at three directions (as shown in Figure 1d) can be observed, generating submicron rhombic or triangular blocks.

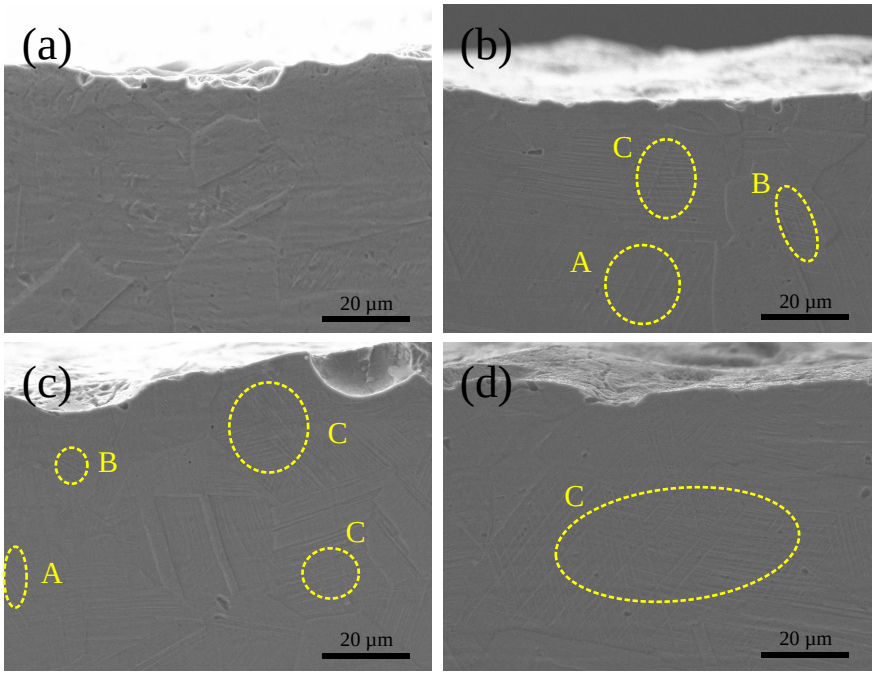

Figure 1. Cross sectional SEM morphologies of grains at various surface conditions: (a) as-received, (b) 100% coverage, (c) 200% coverage, (d) 500% coverage

The conclusion can be drawn that after WSP, microstructure varies with depth from the treated surface and peening coverage because of the deformation twins intersection at different directions, giving rise to plenty of submicron rhombic or triangular blocks, which reveals the original coarse grain refinement induced by WSP.

3.2 Surface roughness

The three-dimensional plots of roughness at the top surface after WSP are shown in Figure 2. Figure 2a clearly shows that the surface of as-received specimen is comparative smooth and the grinded scratches appear in straight lines. After WSP treatment, the grinded scratches disappear and the rough surface is generated by the high speed impact of ceramic balls during WSP process, which are shown in Figure 2b-2d. Table 2 shows the surface roughness values. It is clearly verified that roughness at the top surface increases from 0.314 μm R_a for polished surface to 3.106 μm R_a after WSP with 100% coverage. It can also be seen from the Table 2 that the surface roughness decreases gradually from 3.106 μm R_a to 2.814 μm R_a with increasing the peening coverage from 100% coverage

to 500% coverage, which may be attributed to the more uniform and smoother surface induced by the increased impact duration of shot peening medium for higher peening coverage. The peening coverage can modify the surface roughness effectively, which is also found by Bagherifard et al. [29].

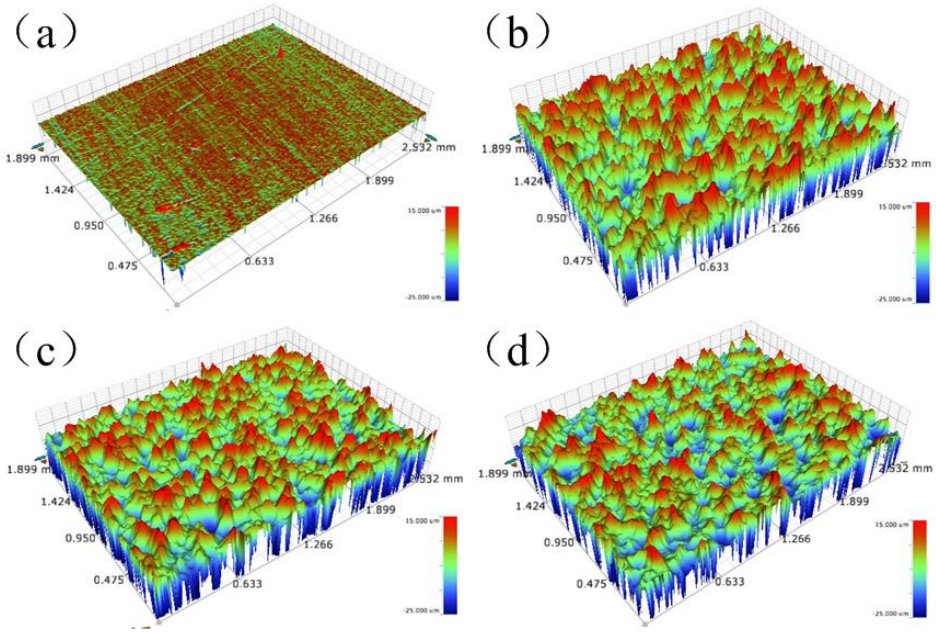

Figure 2. Surface roughness of specimens at various surface conditions: (a) as-received, (b) 100% coverage, (c) 200% coverage, (d) 500% coverage

Table 2. Surface roughness values for different peening conditions

Specimen	As-received	100%	200%	500%
R_a / μm	0.314	3.106	2.92	2.814

3.3 XRD

Figure 3 shows the XRD data of samples in condition of different peening coverage. It is clearly shown that sample before WSP only consists of austenite phase, while the sample treated by WSP shows a mixture of austenite phase and martensite phase. Transformation from austenite to α-martensite can be induced by severe plastic deformation during shot peening treatment [30]. An intense dependence on the intensity of plastic deformation is revealed by the analysis of the volume fraction of α-martensite at the top surface of the wet shot peened samples, which is a function of peening coverage of WSP treatment. According to Eq. 1, the volume fraction V_α can be obtained to be about 34.48% for 100% coverage, 43.18% for 200% coverage and 51.74% for 500% coverage, respectively, implying that the volume fraction of α-martensite increases with the increase of peening coverage.

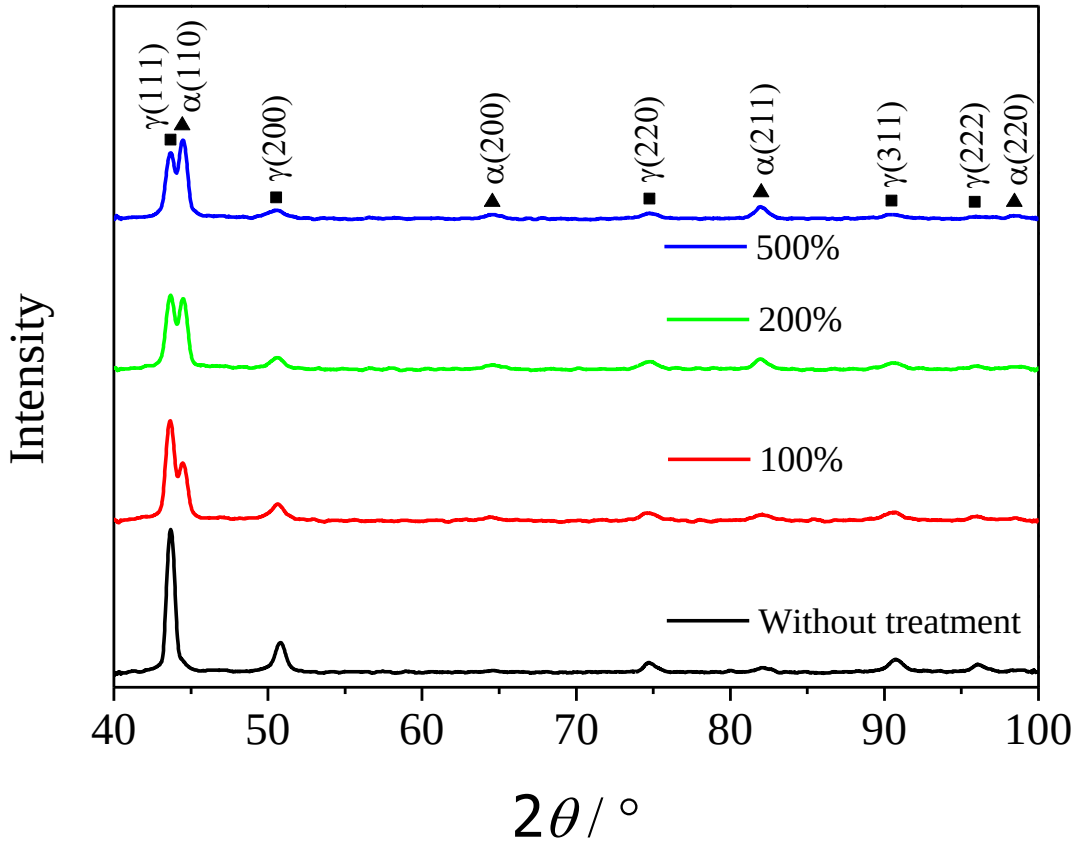

Figure 3. XRD patterns for different peening coverage

3.4 Microhardness

Figure 4 shows the variation of microhardness of the wet shot peened specimens versus distance away from the top surface. It is clearly shown that the profiles reveal an increase in microhardness near the top surface of wet shot peened sample. After WSP treatment, the microhardness reduces rapidly with the increase of depth at first and then goes down slowly until it stays the same at a depth of about 0.45 mm. The maximum microhardness at the top surface induced by 100% coverage WSP is 334.74 HV and increases by 64% compared to 204.16 HV of the base metal. After 500% coverage WSP, the maximum microhardness at the top surface is 384.15 HV and increases by 88.16% compared to that of the base metal. It can be concluded that the strain hardening phenomenon appears because of the plastic deformation during wet shot peening process. The increased microhardness is related with the grain refinement and transformation from austenite to α-martensite induced by the plastic deformation [31]. The microhardness increases with the increase of peening coverage because the intensity of plastic deformation is a function of the peening coverage.

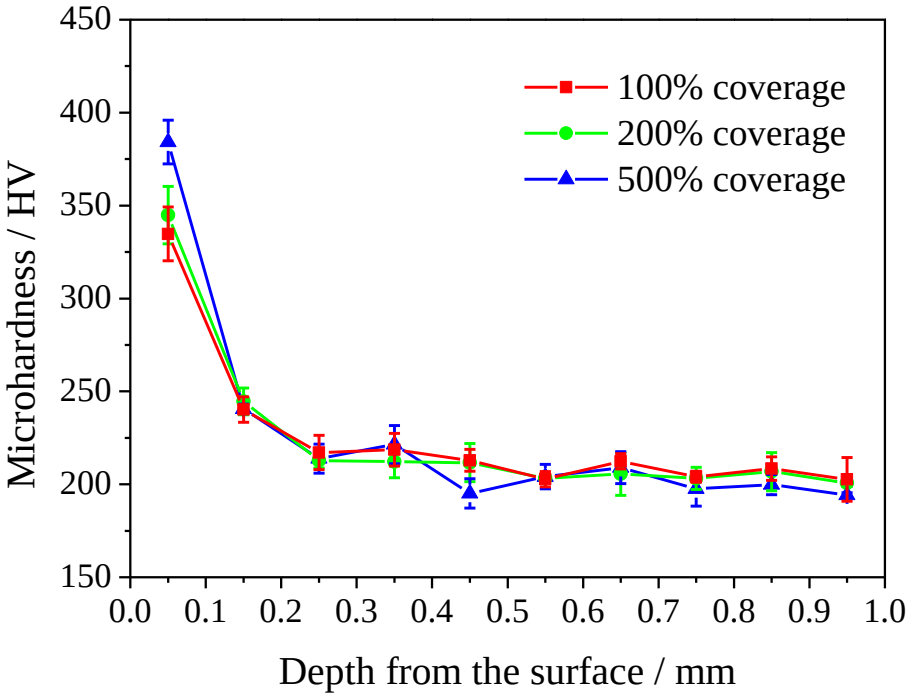

Figure 4. Microhardness distribution in depth for different peening coverage

3.5 Wear behavior

According to Eq. 2, the wear rates of untreated and wet shot peened samples at the 5N load and 20 N load under dry sliding condition are shown in Figure 5. As expected, the untreated AISI 304 stainless steel shows the highest wear rate among all tested samples. When 5 N load is exerted, the average wear rate after 100% coverage WSP has the value of 7.82×10^{-6} $mm^3\cdot N^{-1}\cdot m^{-1}$ and decreases by 33.16% compared to 1.17×10^{-5} $mm^3\cdot N^{-1}\cdot m^{-1}$ of the untreated sample. After 500% coverage WSP treatment, the average wear rate has the value of 7.39×10^{-6} $mm^3\cdot N^{-1}\cdot m^{-1}$ and decreases by 36.84% compared to that of the untreated sample. Exerting the 20 N load makes the wear rates of all samples to increase to 1.56×10^{-5} $mm^3\cdot N^{-1}\cdot m^{-1}$ for the untreated sample, 1.30×10^{-5} $mm^3\cdot N^{-1}\cdot m^{-1}$ for the sample by 100% coverage, 1.28×10^{-5} $mm^3\cdot N^{-1}\cdot m^{-1}$ for the sample by 200% coverage and 1.08×10^{-5} $mm^3\cdot N^{-1}\cdot m^{-1}$ for the sample by 500% coverage, respectively. Compared to the value of wear rate of untreated sample in 20 N load drying sliding condition, the wear rates after 100% coverage and 200% coverage decrease by 16.67% and 17.95%, respectively. However, after 500% coverage WSP, the wear rate decreases by 30.77%, which indicates that high coverage WSP plays a more important role in increasing the wear resistance of AISI 304 stainless steel. When 5 N load is exerted, the samples after WSP show the highest wear resistance improvement and the effect of coverage on wear resistance is less obvious than that of relatively high load of 20 N.

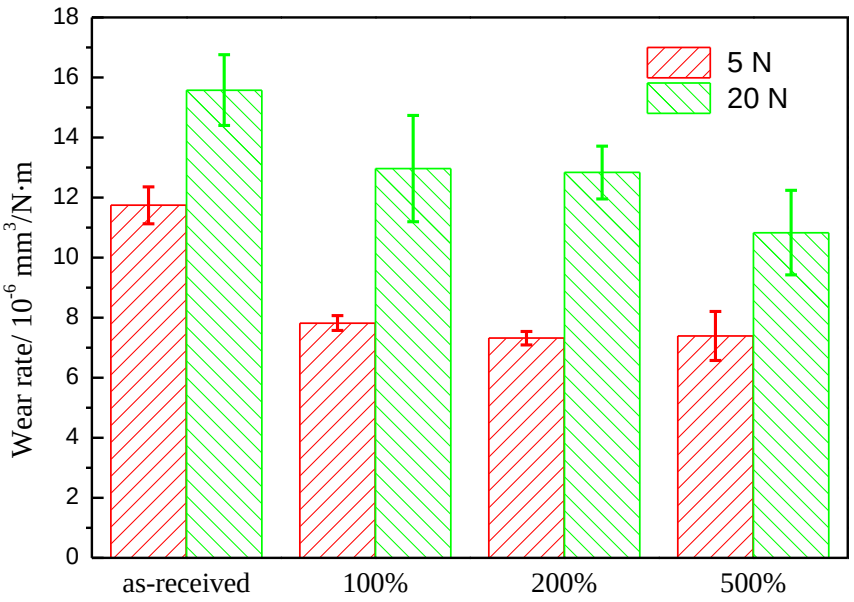

Figure 5. Wear rates of samples with and without WSP

Figure 6 shows the worn tracks of samples before and after wet shot peening at an applied load of 5 N. From Figure 6a-6d, it is clear that sighs of a mixture of abrasive and adhesive wear mechanisms are observed on the worn surface for both as-received and wet shot peened AISI 304 stainless steel. Also, it can be clearly seen in Figure 6 that there are plenty of parallel scratches on the worn surface of all samples and no significant difference in the wear tracks between as-received and wet shot peened samples can be observed, which implies that the abrasive wear mechanism is predominantly for both as-received and wet shot peened AISI 304 stainless steel.

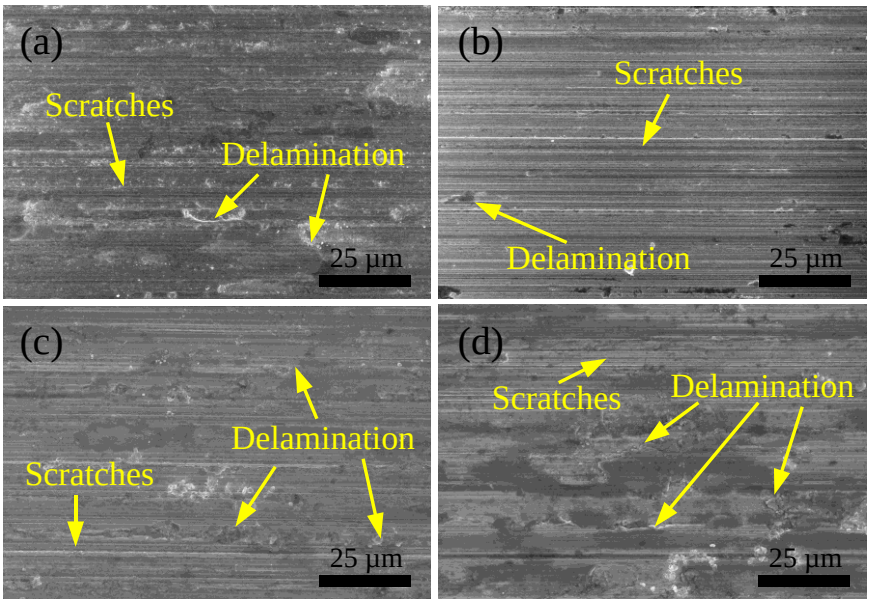

Figure 6. Wear tracks of the worn surfaces at the load of 5 N: (a) as-received, (b) 100% coverage, (c) 200% coverage, (d) 500% coverage

It can be concluded that the remarkable improvement in wear resistance can been achieved after wet shot peening in dry sliding condition, which can be attributed to the higher microhardness of surface layers induced by WSP in comparison to that of as-received sample. Ganesh et al. [15] found that shot peening enhanced sliding wear resistance of titanium alloys by improving the surface hardness. The surface roughness is detrimental to wear performance, which has been reported [32-33]. Compared to results of 100% coverage, wear rates of 200% coverage and 500% are found to reduce due to the decrease in surface roughness and the increase in surface microhardness.

3.6 Corrosion behavior

Figure 7 shows the Nyquist curves of stainless steel with different coverage of WSP treatment. It can be clearly seen that a capacitive arc appears in high frequency region. However, an inductive arc exhibits in low frequency region, implying that pitting corrosion has been initiated at the top surface. Larger diameter of the capacitive arc indicates higher charge transfer resistance and superior corrosion resistance [34]. It is clearly seen that the diameter of the capacitive arc of samples by WSP increase with the increasing peening coverage. After 100% coverage WSP treatment, the capacitive arc diameter is much smaller than that of as-received sample, implying that corrosion resistance after 100% coverage WSP is decreased. However, the capacitive arc diameter of wet shot peened sample with 500% coverage is greatly improved, which implies that corrosion resistance modified by 500% coverage WSP treatment is better than those of lower coverage peened and non-peened samples.

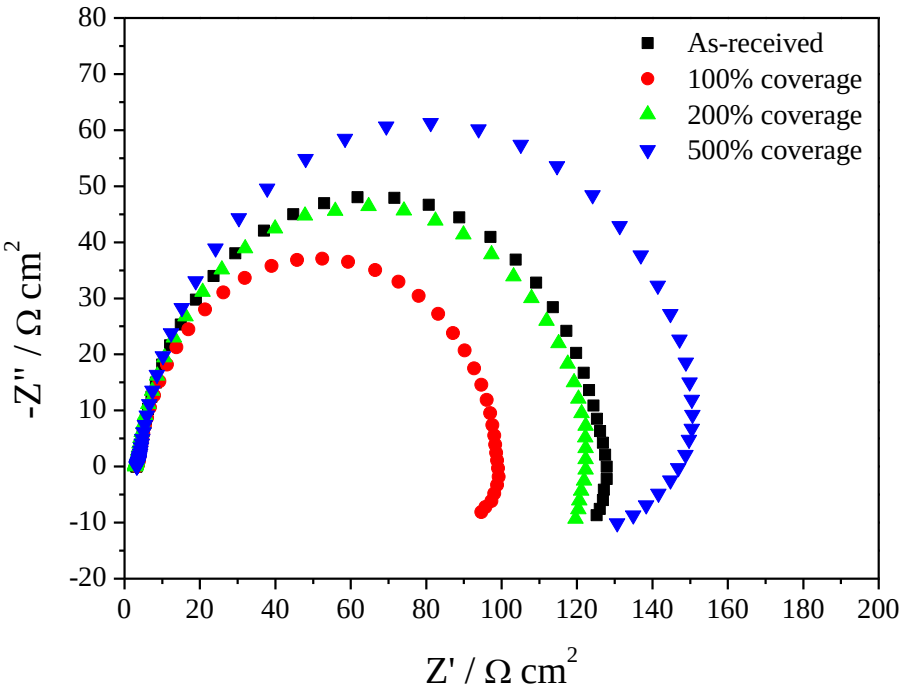

Figure 7. Nyquist plots of samples for different peening coverage

Figure 8 shows the equivalent circuit model proposed for fitting EIS experimental data. In this

model, R_s, R_t and constant phase angle element (CPE) represent solution resistance, charge transfer resistance and double layer capacitance, respectively. L is conductance. R_0 represents resistance associated with passive film growth at pitting initiation region.

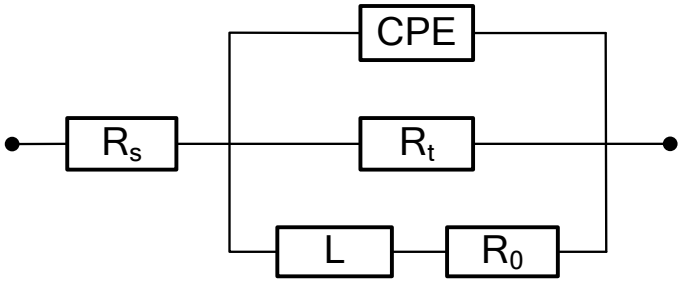

Figure 8. The equivalent circuit model for EIS fitting

The fitted parameters of electrochemical impedance spectroscopy data are listed in Table 3. It can be seen that the charge transfer resistance increases gradually from 96.11 Ω cm^2 to 151.7 Ω cm^2 with increasing the peening coverage from 100% coverage to 500% coverage. Compared to untreated samples, the charge transfer resistance decreases from 125 Ω cm^2 before WSP to 96.11 Ω cm^2 after 100% coverage in 3.5% NaCl + 0.2 mol/L HCl solution. However, 500% peening coverage WSP has a positive effect on the charge transfer resistance by increasing 125 Ω cm^2 to 151.7 Ω cm^2. It is clear that WSP can produce higher charge transfer resistance than that of as-received specimen, which indicates a higher corrosion resistance for high peening coverage WSP because of the formation of the uniform and dense passive film.

Table 3. Fitting electrochemical impedance parameters at room temperature

Sample	R_s / Ω cm^2	CPE		R_t / Ω cm^2	L / H	R_0 / Ω cm^2
		Y_0 / F cm^{-2}	n			
As-received	3.248	0.0003742	0.8516	125	4936	193
100% coverage	3.462	0.0003468	0.8597	96.11	2966	290.7
200% coverage	2.873	0.0003420	0.8532	120.9	4412	359.3
500% coverage	3.407	0.0002713	0.8587	151.7	2112	892.5

The changes of surface characteristics caused by WSP have been used to illuminate the changes of corrosion behavior. For austenitic stainless steels, the density of grain boundaries can be improved by grain refinement, encouraging Cr diffusion to the outside surface and accelerate formation of dense passive film rich in Cr that may acquire a better corrosion resistance [35]. The increased roughness at the top surface and transformation from austenite phase to martensite phase affect the corrosion resistance adversely, which has been reported [24, 36]. Corrosion behavior of stainless steel is determined by the combined action of microstructure, surface roughness and phase transformation. After 500% peening coverage WSP treatment, grain refinement induced by WSP defeats the negative effects resulted from the increased volume fraction of martensite and surface roughness. But the higher

surface roughness and generation of martensite phase would enhance the adverse effects and reduce corrosion resistance when 100% peening coverage is employed.

4. CONCLUSIONS

The influences of surface characteristics induced by wet shot peening on wear and corrosion resistance of stainless steel have been studied by dry sliding wear tests and EIS experiments. Surface characteristics, such as microstructure, surface roughness, microhardness and martensite phase transformation are analyzed. The results are listed in the following:

(1) Deformation twins with gradient variation appear near the surface layer treated by wet shot peening presents and is affected by peening coverage, which result in original coarse austenitic grain refinement.

(2) Surface roughness can be increased by wet shot peening, which varies from 0.314 μm R_a for polished surface to about 3.106 μm R_a after 100% coverage wet shot peening. Phase transformation from austenite phase to martensite phase occurs after WSP. The volume fraction of α-martensite of wet shot peened sample is strongly dependent on the intensity of plastic deformation, which is a function of peening coverage.

(3) Surface microhardness can be enhanced significantly due to the strain hardening produced by WSP. The maximum microhardness after WSP increase by 64% for 100% coverage and 88.16% for 500% coverage compared to 204.16 HV of the base metal, respectively.

(4) The remarkable improvement in wear resistance can been achieved after wet shot peening in dry reciprocating sliding condition. The wear mechanism is a mixture of abrasive and adhesive wear for both as-received and wet shot peened AISI 304 stainless steel. The highest wear resistance improvement after WSP can be obtained at a low applied load and the effect of coverage on wear resistance is more obvious at a relatively high applied load.

(5) The influence of wet shot peening on corrosion behavior is controlled by the combined action of grain refinement, surface roughness and deformation induced martensite. The charge transfer resistance of sample treated by relative higher peening coverage is larger than those of lower peening coverage treated and as-received sample at room temperature, which indicates the corrosion resistance of materials could be improved for the relative higher peening coverage WSP.

ACKNOWLEDGEMENTS

The financial supports of the Jiangsu Innovation Project for Marine Science and Technology (Grant No. HY2017-10), the Natural Science Foundation of the Jiangsu Higher Education Institutions of China (Grant No. 18KJB430030), Special Cooperation between City and School of Yangzhou (Grant No. YZ2018210), Natural Science Foundation of Jiangsu Province (Grant No. BK20190915), Postgraduate Research & Practice Innovation Program of Jiangsu Province (Grant No. SJCX18_0797) are gratefully acknowledged by the authors.

References

1. F. Arjmand, A. Adriaens, *Int. J. Electrochem. Sc.*, 7(2012)8007.
2. M. Ebrahimi, S. Amini, S. M. Mahdavi, *Int. J. Adv. Manuf. Technol.*, 88(2017)1557.
3. O. M. Alyousif, R. Nishimura, *Corros. Sci.*, 50(2008)2919.
4. H. S. Costa-Mattos, I. N. Bastos, J. A. C. P. Gomes, *Corros. Sci.*, 50 (2008) 2858.
5. P. D. Tiedra, O. Martin, *Mater. Design*, 49(2013)103.
6. A. A. Aghuy, M. Zakeri, M. H. Moayed, M. Mazinani, *Corros. Sci.*, 94 (2015) 368.
7. L. Ceschini, C. Chiavari, E. Lanzoni, C. Martini, *Mater. Design*, 38(2012)154.
8. Y. Sun, T. Bell, *Wear*, 253(2002)689.
9. Y. Sano, M. Obata, T. Kubo, N. Mukai, M. Yoda, K. Masaki, Y. Ochi, *Mat. Sci. Eng. A-Struct.*, 417(2006)334.
10. X. L. Wei, X. Ling, *Appl. Surf. Sci.*, 301 (2014) 557.
11. X. L. Wei, C. Zhang, X. Ling, *J. Alloy. Compd.*, 723 (2017) 237.
12. S. Kumar, K. Chattopadhyay, V. Singh, *J. Alloy. Compd.*, 724 (2017) 187.
13. D. J. Chadwick, S. Ghanbari, D. F. Bahr, M. D. Sangid, *Fatigue Fract. Eng. M.*, 41 (2018) 71.
14. G. Q. Chen, Y. Jiao, T. Y. Tian, X. H. Zhang, Z. Q. Li, W. L. Zhou, *Trans. Nonferrous Met. Soc. China*, 24 (2014) 690.
15. B. K. C. Ganesh, W. Sha, N. Ramanaiah, A. Krishnaiah, *Mater. Design*, 56 (2014) 480.
16. S. Mitrovic, D. Adamovic, F. Zivic, D. Dzunic, M. Pantic, *Surf. Sci.*, 290 (2014) 223.
17. V. Fridrici, S. Fouvry, P. H. Kapsa, *Wear*, 250 (2001) 642.
18. A. Zammit, S. Abela, L. Wagner, M. Mhaede, M. Grech, *Wear*, 302 (2013) 829.
19. T. S. Wang, J. K. Yu, B. F. Dong, *Surf. Coat. Tech.*, 200 (2006) 4777.
20. X. D. Chen, Y. S. Li, Y. T. Zhu, Y. K. Bai, B. Yang, *Appl. Surf. Sci.*, 481 (2019) 1305.
21. H. Kovaci, Y. B. Bozkurt, A. F. Yetim, M. Aslan, A. Celik, *Surf. Coat. Tech.*, 360 (2019) 78.
22. A. A. Ahmed, M. Mhaede, M. Wollmann, L. WagnerInstitute, *Appl. Surf. Sci.*, 363 (2016) 50.
23. X. L. Wei, D. J. Zhu, X. Ling, L. Yu, M. Dai, *Int. J. Electrochem. Sci.*, 13 (2018) 4198.
24. H. S. Lee, D. S. Kim, J. S. Jung, Y. S. Pyoun, K. Shin, *Corros. Sci.*, 51 (2009) 2826.
25. U. Zupanc. J. Grum, *J. Mater. Process Tech.*, 210 (2010) 1197.
26. A. K. De, D. C. Murdock, M. C. Mataya, J. G. Speer, D. K. Matlock, *Scripta Mater.*, 50 (2004) 1445.
27. B. N. Mordyuk, G. I. Prokopenko, M. A. Vasylvev, M. O. Lefimov, *Mat. Sci. Eng. A*, 458 (2007) 253.
28. M. Jayalakshmi, P. Huilgol, B. R. Bhat, K. U. Bhat, *Surf. Coat. Tech.*, 344 (2018) 295.
29. S. Bagherifard, R. Ghelichi, M. Guagliano, *Appl. Surf. Sci.*, 258 (2012) 6831.
30. Y. S. He, K. B. Yoo, H. Y. Ma, K. Shin, *Mater. Lett.*, 215 (2018) 187.
31. M. Chen, H. B. Liu, L. B. Wang, Z. Xu, V. Ji, C. H. Jiang, *Appl. Surf. Sci.*, 459 (2018) 155.
32. K. H. S. Silva, J. R. Carneiro, R. S. Coelho, H. Pinto, P. Brito, *Wear*, 440 (2019) 203099.
33. P. L. Menezes, S. V. Kailas, *Wear*, 267 (2009) 1534.
34. W. Ye, Y. Li, F. H. Wang, *Electrochim. Acta*, 51 (2006) 4426.
35. W. Ye, Y. Li, F. H. Wang, *Electrochim. Acta*, 54 (2009) 1339.
36. A. Barbucci, M. Delucchi, M. Panizza, M. Sacco, G. Cerisola, *J. Alloy. Compd.*, 607 (2001) 317.

© 2020 The Authors. Published by ESG (www.electrochemsci.org). This article is an open access article distributed under the terms and conditions of the Creative Commons Attribution license (http://creativecommons.org/licenses/by/4.0/).